MICROSTRUCTURAL CHARACTERIZATION OF MATERIALS BY A RAYLEIGH WAVE ANALYSIS

F. Tardy, M.H. Nadal,C. Gondard, L. Paradis
CEA DRMN/MOS
BP12
F- 91680 BRUYERES LE CHATEL
France

P. Guy, J. C. Baboux
INSA/GEMPPM
F- 69621 VILLEURBANNE
France

INTRODUCTION

It is well known that material characteristics properties such as anisotropy, grain size, damage, roughness, can affect the Rayleigh wave propagating on a sample surface. The acoustic microscopy using broad-band pulses is one of the methods which can generate Rayleigh waves in a simple way. The acoustic energy generated by a transducer in the coupling medium reaches the sample surface and is partially reflected into an axial echo and converted into a Rayleigh wave at the Rayleigh critical angle θ_R. With an impulse excitation, these two echoes are resolved in time. In this case, the Rayleigh velocity can be also obtained through a time of flight measurement. One of the challenge of this technique is to be able to perform time measurements with the necessary accuracy in order to detect shifts in the material properties.

V(Z) TECHNIQUES IN BROAD-BAND MODE

Usually, acoustic microscopes exploit interferences between waves obtained with resonant transducers excited by narrow-band tone bursts. A well known approach relies on the determination of the V(z) curve, also called the acoustic signature of a material. However, if a pulse excitation (broad-band mode) is used, the Rayleigh contribution is thus time resolved [1], [2]. Consequently, independent measurement of the longitudinal wave velocity in water V_O and Rayleigh wave velocity V_R on the material are performed.

Review of Progress in Quantitative Nondestructive Evaluation, Vol. 16
Edited by D.O. Thompson and D.E. Chimenti, Plenum Press, New York, 1997

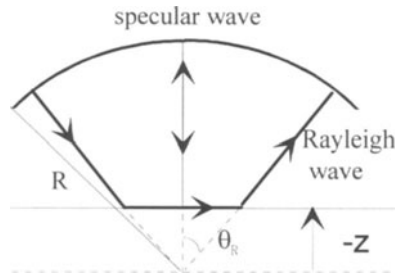

Figure 1. Ray model used for the evaluation of the time of flight t_o and t_R.

It allows an automatic correction on V_R if V_o is modified in case of temperature fluctuations.

The piezoelectric elements used in this study are spherical or cylindrical which radiate directly into water [3], and thus constitute an aberration free surface that focuses the emitted acoustic beam into a diffraction limited spot (or line) at the center of curvature of the transducer. In order to separate the axial wave and the leaky surface wave in the time domain, the transducer must be sufficiently close to the sample surface. The arrival times $t_o(z)$ and $t_R(z)$ of the two components are derived from the ray model described on figure 1, and given in expressions (1) and (2).

$$t_o(z) = \frac{2R}{V_o} + \frac{2z}{V_o} \tag{1}$$

$$t_R(z) = \frac{2R}{V_o} + \frac{2z}{V_o}\sqrt{1-\left(\frac{V_o}{V_R}\right)^2} \tag{2}$$

From (1) and (2) we derive a procedure to evaluate the material Rayleigh wave velocity. The signal including the specular and Rayleigh components is stored for multiple z positions. The signal collected at the first position z_o is taken as a reference. Arrival time measurements are first performed on the specular wave and next, on the Rayleigh waves and plotted versus z. The intercorrelation technique has been selected for its better accuracy. The slope of expressions (1) and (2) gives V_o and V_R. By this way, we are able to measure the absolute Rayleigh wave velocity with an accuracy better than 0.6%. Moreover, by comparing the arrival time of the Rayleigh echo at the same z position for several material properties, we can measure velocity variation better than 0.15%.

Now, this technique is used to show material properties variations due to texture effects or grain size.

TEXTURE ANISOTROPY DUE TO ROLLING :

Austenitic stainless steel samples of initial thickness of 10 mm were rolled up to the final thickness of 5 mm at room temperature. A single direction (1D) rolling and a two directions (2D) rolling are successively studied. The line focus beam acoustic transducer system is applied to investigate the elastic properties of the rolled specimens. Unlike point focus acoustic microscopy, which integrates the acoustic properties over all radial directions, this configuration allows the measurement of the Rayleigh wave velocity in specified directions.

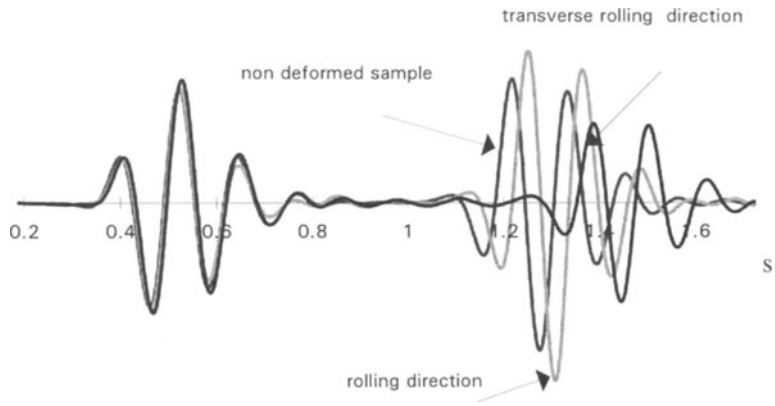

Figure 2. Texture effect on the signal.

The center frequency of the transducer used in this study is 10 MHz and the radius of curvature is 10 mm. Figure 2 shows several signals stored at the same z position for a non deformed and a (1D) rolled specimen. The arrival time of the specular wave depends only of the z position whereas the arrival time of the Rayleigh wave depends of the material elastic constants and the propagation directions in case of anisotropy.

Assuming that the material is not strongly anisotropic, we can study the propagation of the Rayleigh waves with the perturbation formalism by computing the elastic constants variations C'_{km} defined by :

$$C'_{km} = C_{km} - C^{i}_{km} \tag{3}$$

C^{i}_{km} and C_{km} are the elastic constants of the isotropic and textured samples respectively.

Delsanto [4] derives the Rayleigh wave phase velocity as a function of the propagation direction and the elastic constants for the special case of slight orthotropy. By taking into account the symmetry properties of the cubic crystallites and of the orthorhombic symmetry of the sample, the coefficient C'_{km} are dependent on each other [5] :

$$\begin{aligned} &C'_{44} = C'_{23},\ C'_{55} = C'_{13},\ C'_{66} = C'_{12} \\ &C'_{11} + C'_{12} + C'_{13} = 0 \\ &C'_{12} + C'_{22} + C'_{23} = 0 \\ &C'_{13} + C'_{23} + C'_{33} = 0 \end{aligned} \tag{4}$$

It is then concluded that, for rolling texture of cubic metals, there are only three independent texture parameters C'_{km}. Finely, the relative velocity variation $v_R(\theta) - v^{i}_R$ as a function of the propagation direction is given by:

$$v_R(\theta) - v_R^i = A_1 (C'_{13} + C'_{23}) + A_2 (C'_{23} - C'_{13}) \cos 2\theta + A_3 (-8C'_{12} - C'_{23} - C'_{13}) \cos 4\theta \quad (5)$$

where v_R^i is the Rayleigh wave velocity in the isotropic non deformed specimen and A_1, A_2 ,A_3 are constants which depend on the density and the elastic constants of the isotropic material. By extrapolating the experimental curve $v_R(\theta) - v_R^i$, we can derive the elastic constants of the textured material with (5).

Velocity measurements were performed as a function of the wave propagation direction. Figure 3.a. shows the measured Rayleigh wave velocity variation $v_R(\theta) - v_R^i$ obtained on a (1 D) rolled sample. The propagation direction of zero degree corresponds to the rolling direction. Figure 3.b shows the Rayleigh wave velocity measured on a (2 D) rolled sample. Compared to figure 3.a, the velocity variation is smaller. In this case, we note a 60 degrees rotation of the principle axes.

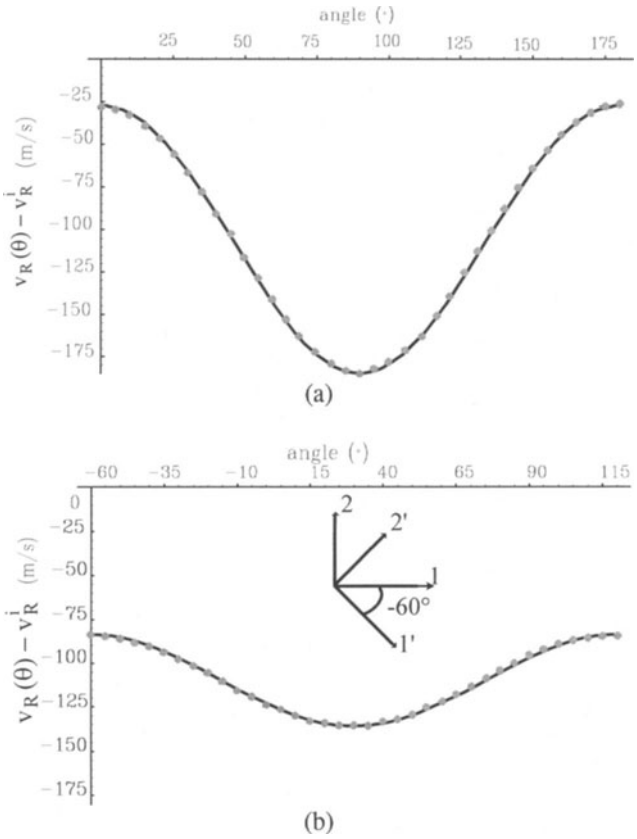

Figure 3 . Rayleigh velocity variation. (a) rolling in a single direction, (b) rolling in two directions. —— theoretical curve, ● experimental data.

Table 1. Elastic constants C'_{km} (GPa) for rolled steel sample. (a) 1D, (b) 2D

$$\begin{bmatrix} 0\pm2 & 5\pm0.5 & -5\pm3 & 0 & 0 & 0 \\ 5\pm0.5 & 15\pm5 & -20\pm5 & 0 & 0 & 0 \\ -5\pm3 & -20\pm5 & 25\pm7 & 0 & 0 & 0 \\ 0 & 0 & 0 & -20\pm5 & 0 & 0 \\ 0 & 0 & 0 & 0 & -5\pm3 & 0 \\ 0 & 0 & 0 & 0 & 0 & 5\pm0.5 \end{bmatrix}$$

(a)

$$\begin{bmatrix} 7\pm2 & 3.5\pm0.5 & -10.5\pm3 & 0 & 0 & 0 \\ 3.5\pm0.5 & 12\pm5 & -15.5\pm5 & 0 & 0 & 0 \\ -10.5\pm3 & -15.5\pm5 & 26\pm7 & 0 & 0 & 0 \\ 0 & 0 & 0 & -15.5\pm5 & 0 & 0 \\ 0 & 0 & 0 & 0 & -10.5\pm3 & 0 \\ 0 & 0 & 0 & 0 & 0 & 3.5\pm0.5 \end{bmatrix}$$

(b)

In order to evaluate C'_{km} , we also need to measure the absolute Rayleigh velocity v_R on the non deformed specimen and for the deformed specimen in a single direction, for example at zero degree which gives $v_R(0)$.The elastic constants variations C'_{km} have been computed and are given in table 1.

GRAIN SIZE EFFECTS

The (2D) rolled samples were submitted to heat treatments in order to get three samples with an average grain-size equal to $d_1=10$ μm, $d_2=40$ μm and $d_3=100$ μm. Comparatively to the previous samples, the heat treatment involves the destruction of any texture. Optical micrographies have been performed to check the homogeneity of the grain size and the lack of specific orientations. The signals were stored with a spherical shaped transducer of 10 mm radius of curvature and a 20 MHz center frequency.

We observe a significant decrease of the amplitude of the Rayleigh echo due to the increasing grain-size (Fig. 4.a), whereas the specular echo is the same in each case. Moreover, the arrival time of the Rayleigh echo depends on the grain-size : the corresponding velocity is smaller when this last one increases.

To model this effect, we first need to compute accurately the ultrasonic signal constituted by the two main echoes (specular and Rayleigh). This modeling has been developed by taking into account the broadband pulse, the complex radiated field of the transducer and its interaction with the material which is given by the reflectance function $R(\theta)$.

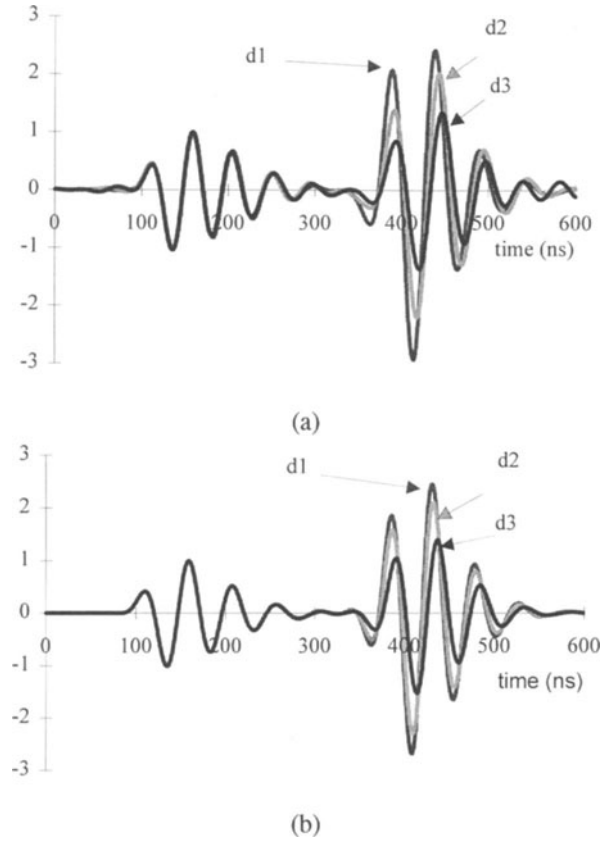

Figure 4. Grain size effect on the Rayleigh echo at z=-1.4mm. (a) experimental and (b) simulated signals.

We just remind that R(θ) is a function of the material and liquid densities, the velocity in the liquid, and the velocities v_L and v_T of the longitudinal and shear waves in the solid. This modeling has been tested for different materials where attenuation can be neglected [6]. Now, in the case of dispersive materials, the wavenumbers k_L and k_T of the longitudinal and transverse waves become complex :

$$k_L^* = k_L - j\alpha_L \qquad k_T^* = k_T - j\alpha_T \tag{6}$$

where α_L and α_T are the attenuation coefficients of the longitudinal and shear waves.

Eq (6) yields to complex velocities :

$$v_T^* = v_T - j\alpha_T \frac{v_T^2}{2\pi f} \qquad v_L^* = v_L - j\alpha_L \frac{v_L^2}{2\pi f} \tag{7}$$

Using this velocities in the reflectance function, we can take into account the attenuation coefficients in the modeling, knowing that the Rayleigh-wave attenuation coefficient is a function of α_L and α_T.

To describe accurately the experimental signals, we need to evaluate α_L and α_T. It is shown that the amplitude of the Rayleigh wave is stronger affected by the α_T coefficient than by the α_L coefficient. This effect is quite similar to the v_R dependence versus v_L and v_T.

Our method consists in fitting the theoretical signals to the experimental one by a recurrent approach of the α_L and α_T coefficients. This is performed considering that $\lambda \approx 2\pi d$, which involves a linear dependence of $\alpha_{L,T}$ versus the grain-size ($\alpha \propto d.f^2$)

The attenuation coefficients are given in the following table :

Table 2 . Attenuation coefficient at 20 MHz

in size (μm)	10	40	100
α_T (dB/m)	870 ± 170	1980 ± 170	4570 ± 170

The figure 4.b shows the theoretical result which is in good agreement with the experimental data (Fig. 4.a).

CONCLUSION

We have presented the Surface Acoustic Microscopy technique in the case of a broadband pulse excitation. This technique enables quantitative relations between Rayleigh velocity measurements and the elastic constants for textured material. We also measured the attenuation effects as a function of the grain size and our modeling describes accurately the experimental signals. Those results demonstrate the accuracy of the acoustic microscopy technique using a broad band pulse excitation.

REFERENCES

1. Kazushi Yamanaka. J. Appl. Phys. 54 (8), August 1983.
2. J.Zhang, J.C. Baboux and P.Guy. IEEE Ultrasonics symposium. Cannes, November 517-520, 1994.
3. Kenneth K. Liang, Gordon S. Kino and Butrus T. Khuri-Yakub. IEEE transactions on sonics and ultrasonics. Volume SU-32, number 2, March 1985.
4. C.M. Sayers. Ultrasonic velocities in anisotropic polycrystalline aggregates. J. Phys. D : Appl. Phys., 15 (1982) pp 2157-2167.
5. P.P. Delsanto, A.V. Clark, Jr. Rayleigh wave propagation in deformed orthotropic materials. J. Acoust. Soc. Am 81(4). April 1987.
6 C. Gondard, F. Tardy, M.-H. Noroy-Nadal, L. Paradis and J.C. Baboux, Review of Progress in QNDE, Vol. 15B, pp 1605-1612, 1995.